International Journal of Infrared and Millimeter Waves, Vol. 22, No. 1, 2001

FAST PHYSICAL OPTICS SIMULATIONS OF THE MULTI-BEAM DUAL-REFLECTOR SUBMILLIMETER-WAVE TELESCOPE ON THE ESA PLANCK SURVEYOR

Vladimir Yurchenko,[1,2] John Anthony Murphy,[1] and Jean-Michel Lamarre[3]

[1]*Experimental Physics Department*
National University of Ireland
Maynooth, County Kildare, Ireland
[2]*Institute of Radiophysics and Electronics*
National Academy of Sciences of Ukraine
12 Proskura Street
Kharkov, 61085, Ukraine
[3]*Institut d'Astrophysique Spatiale*
Universite de Paris XI
bat. 121, Orsay Cedex, Paris, 91405, France

Received October 25, 2000

Abstract

We present physical optics simulations of the multi-beam dual-reflector submillimeter-wave telescope on the ESA PLANCK surveyor designed for measuring the temperature anisotropies and polarization characteristics of the cosmic microwave background. The telescope is of a non-conventional Gregorian configuration, with two ellipsoidal reflectors providing a very large field of view at the focal plane where the array of 76 horn antennas feeding low-temperature detectors is located. We analyse the defocusing effects of the system, the polarization properties of the telescope, and the optical performance of the high-frequency channels based on special multi-moded horns operating at 545 and 857 GHz.

Key words: physical optics, submillimeter waves, polarization, dual reflector, ESA PLANCK Surveyor

0195-9271/01/0100-0173$19.50/0

1. Introduction

The ESA PLANCK surveyor is being designed for imaging the temperature anisotropies and polarization characteristics of the cosmic microwave background over the whole sky with unprecedented sensitivity, accuracy and angular resolution using nine frequency channels ranging between 25 and 1000 GHz [1].

To achieve this goal, the PLANCK surveyor utilizes a special dual-reflector submillimeter-wave telescope of a non-conventional Gregorian configuration. Both the design and simulation of such a telescope are extremely challenging. Firstly, the telescope is electrically large, the primary mirror having a projected aperture diameter of D=1500 mm while the minimal wavelength involved is only about λ=0.3 mm (i.e., D/λ=5000). Secondly, it is an axially asymmetric system that consists of two essentially defocused ellipsoidal reflectors providing a very large field of view at the focal plane where the array of 76 horn antennas feeding low-temperature detectors is located. To add to the complexity, the 14 channels operating at the highest frequencies of 545 and 857 GHz are based on multi-moded horns [2] designed for receiving maximum microwave power within the required angular resolution of 5 arcminutes on the sky. The polarization characteristics of the microwave background should be measured in different channels as well.

Among various simulation techniques, physical optics is the most adequate one for the comprehensive analysis of the given system [3, 4]. However, conventional implementations of the technique do not fit the size of the problem. For example, even the best commercial software requires about one week of computation of the main beam at the relatively low frequency of f=143 GHz, while all conventional physical optics codes collapse at the highest frequencies f=545 – 857 GHz.

Our implementation of the technique overcomes the limitations of a generic approach for large multi-reflector systems and can perform typical simulations of the telescope in the order of minutes. In particular, it requires only 2 minutes for computing the main beam of the Gaussian horn at the frequency f=143 GHz and about 20 minutes for the beam of six modes of the multi-moded horn at f=545 GHz using a PC Pentium III (500 MHz) under the Linux operating system.

The aim of this paper is to present the main results of our simulations concerning (1) the measurement of polarization with tilted off-axis dual-reflector Gregorian telescope and (2) the propagation of multi-moded beams through such a complicated quasi-optical system.

2. Geometry of the Telescope and Detector Unit

A general view of the Planck telescope is shown in Fig. 1 and a view of the entrance horns of the High-Frequency Instrument (HFI), as seen from the telescope, is given in Fig. 2 [5].

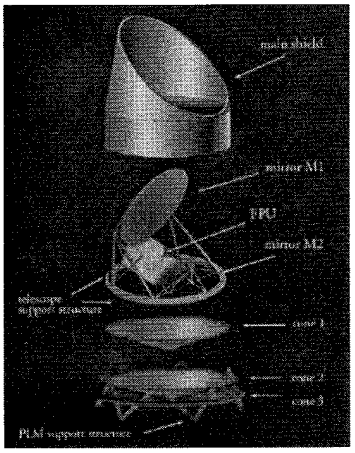

Fig. 1: A view of the Planck telescope

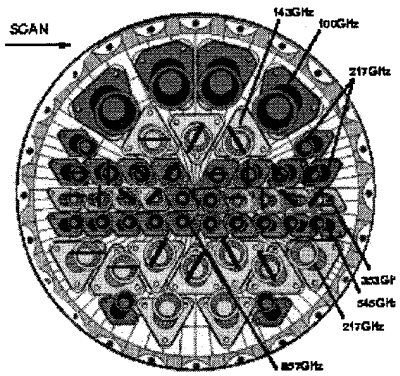

Fig. 2: Entrance horns of HFI

In this paper, we consider the power patterns, polarization characteristics and defocusing effects of the two beams that correspond to the horns H-143-4 (f =143 GHz) and H-545-1 (f =545 GHz), the ones on the extreme left of the second and the fourth rows from the bottom in Fig. 2 (notations in Fig. 2 and some parameters in [1] are out of date).

H-143-4 is a Gaussian horn with the electric field at the aperture being linearly polarized and given by the formula

$$\vec{E}(r) = E_0 \exp(-r^2 / w_0^2)\, \vec{e}_0 \qquad (1)$$

where r is the radial coordinate, $w_0 = 3.289$ mm is the half-waist of the beam, $a = 5$ mm is the aperture radius and $\vec{e}_0$ is the polarization vector.

H-545-1 is a multi-moded conical horn, with the electric field at the aperture given by the set of six modes ($m = 1..6$) defined as follows

$$\vec{E}_m(r,\varphi) = E_{0m}\, J_n(p_m r / a) \exp(-iqr^2)\, \vec{e}_m(\varphi) \qquad (2)$$

where $J_n(.)$ is the Bessel function, $n = 0, 1, 2$ when $m = 1$ or 6, 2 or 3, and 4 or 5, respectively, $a = 4.1$ mm, $p_1 = 2.405$, $p_2 = p_3 = 3.831$, $p_4 = p_5 = 5.136$, $p_6 = 5.520$, $q = \pi / \lambda L$, $L = 28$ mm is the length of the horn, and $\vec{e}_m(\varphi)$ is the polarization vector depending on the azimuthal angle, $\vec{e}_{1,6}=\hat{j}$, $\vec{e}_{2,3} = \pm\sin(\varphi)\hat{i}+\cos(\varphi)\hat{j}$, and $\vec{e}_{4,5} = \sin(2\varphi)\hat{i} \pm \cos(2\varphi)\hat{j}$ ($E \sim \exp(i\omega t)$). Amplitudes E_0 and E_{0m} in (1) and (2) are normilized so that each mode has the total power $P = 1$.

Horn positions and orientations are specified with respect to the reference detector plane P defined as a plane normal to the chief ray at the (0,0) point, which is the paraxial focus of the telescope. When studying defocusing effects, we have the horn axis fixed. The geometrical focus of the horn, F, is specified by the refocus parameter R_F defined as a distance from the plane P to the point F measured along the horn axis, with $R_F > 0$ when moving towards the secondary mirror. Optimum 'geometrical' values of R_F have been provided as a result of the previous design performed with ray tracing software. For the horns H-143-4 and H-545-1, they are $R_F = 10.5$ mm and $R_F = 5.526$ mm, respectively.

3. Beam from the Gaussian horn H-143-4

Fig. 3 shows the power pattern of the telescope beam from the Gaussian horn H-143-4 as projected on the plane normal to the telescope line-of-sight at the (0, 0) point (α_x and α_y are the horizontal and vertical axes on the plane, respectively, measured in degrees). The beam is perfectly shaped down to –30 dB below the maximum. Even though being slightly elliptical (the ellipticity is 1.19), it can be fairly well approximated by a Gaussian function with a full beam width of $W_{\min} = 9.3$ arcmin and $W_{\max} = 11.1$ arcmin at –4.3 dB and the average full beam

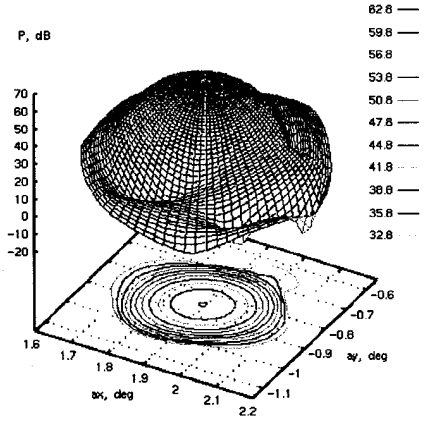

Fig. 3: Power pattern of the beam H-143-4

width of about $W_0 = 10.2$ arcmin at –4.3 dB and $W = 8.5$ arcmin at –3 dB.

The polarization of the beam is generally elliptical except precisely at the beam axis where it remains linear. In order to achieve the required orientation of the polarization pattern in the sky, we should orient the polarization vector $\vec{e}_0$ properly on the horn aperture.

For immediate comparison of polarizations measured by different horns when scanning through the sky, we should use easily aligned directions in the sky as equivalent reference polarization axes for different beams. Such directions are the meridians in the spherical frame of the telescope, with the telescope spin axis being the pole (the meridians define local verticals at various observation points, while the parallels are local horizontals that constitute the orthogonal directions).

Also, we should properly define the reference axis for polarization vectors $\vec{e}_0$ of differently tilted horns. We define the reference axis as the direction of $\vec{e}_0$ in the horn aperture plane that is projected on the vertical axis in the detector plane P. The orientation of $\vec{e}_0$ is specified by the angle φ_e in the horn aperture plane measured from this reference in a clockwise direction when looking from the horn to the secondary mirror.

Using these definitions, we have found that the beam of the H-143-4 horn is vertically polarized at its axis (the electric field is directed along the meridian) if the horn polarization vector $\vec{e}_0$ is specified by the angle $\varphi_e = 3.07$ deg.

The deviation of the major axis of the polarization ellipse from the local meridian as a function of the observation point within the beam is shown in Fig. 4.

When the polarization is properly adjusted, the cross-polarized component of the field measured with respect to the given direction is minimized. For example, in the case of vertical polarization discussed above,

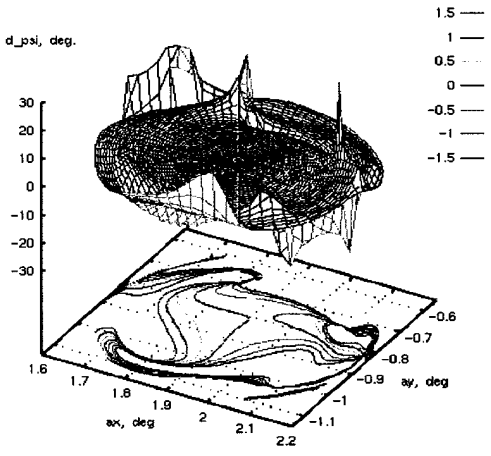

Fig. 4: Deviation of the major axis of polarization ellipse from the local meridian as a function of the observation point within the beam ($\varphi_e = 3.07$ deg)

the power pattern of the cross-polarized (horizontal) component of the electric field is shown in Fig. 5. The pattern can be approximated as

$$P_{cr}(\vartheta,\varphi) = P_{cr0}\,[(\theta/\theta_0)\sin(\varphi-\varphi_0)]^p \exp[-(\theta/\theta_0)^q] \qquad (3)$$

where $P_{cr0} = 28\,\text{dB}$ is the maximum power of the cross-polarized field at the points specified by the polar angle $\theta_0 = 0.09\,\text{deg}$ and the azimuthal angles $\varphi_0 \pm 90$ deg ($\varphi_0 = 8\,\text{deg}$) measured from the centre of the pattern at $\alpha_x = 1.9\,\text{deg}$, $\alpha_y = -0.85\,\text{deg}$, with the exponents being $p = 1.5$ and $q = 3.5$ (the values of the parameters depend on the position of the horn considered).

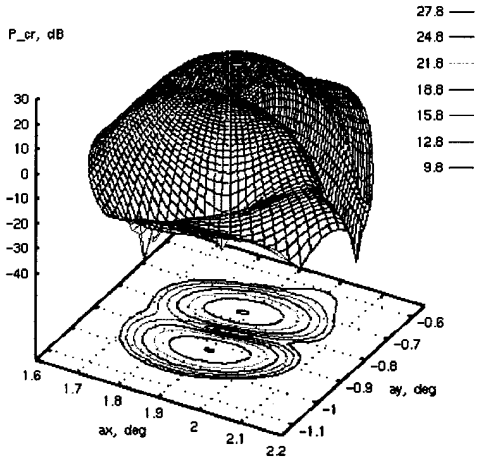

Fig. 5: Power pattern of the horizontal (cross-polarized) component of the vertically polarized beam from the Gaussian horn H-143-4 when $\varphi_e = 3.07$ deg

Fig. 5 resembles very much the power pattern of the minor axis of the polarization ellipse, being only somewhat greater in magnitude at the points where the polarization ellipse is more tilted with respect to the local meridian.

Observing Figures 3 and 5, one can see that the cross-polarizied component in this case is about –35 dB below the co-polarized one (the latter constitutes the main power of the beam).

For comparison, if the polarization vector $\vec{e}_0$ is not properly adjusted ($\varphi_e = 0$), the measured horizontal component (being incorrectly interpreted as the 'cross-polarized' field) is about 10 dB greater than the absolute possible minimum.

Other essential data concerning the polarization properties of the beam are presented in Figures 6 and 7. Fig. 6 shows that the ratio of the minor-to-major axes of the polarization ellipse is well below 0.1 in the central part of the beam where the total power drops down by about 20 dB. Fig. 7 shows that the sense of polarization changes when crossing the horizontal

centre line of the beam being in full agreement with the cross-polarization pattern shown in Fig. 5.

Notice, however, that the structure of all the patterns above depends on the position of the particular horn. For example, if the centre of the horn aperture is placed at the paraxial focus of the telescope, the centre line of the cross-polarization pattern becomes vertical instead of being horizontal as in Figures 5 to 7 (the parameter φ_0 in the approximation (3) is $\varphi_0 = 90\,\text{deg}$).

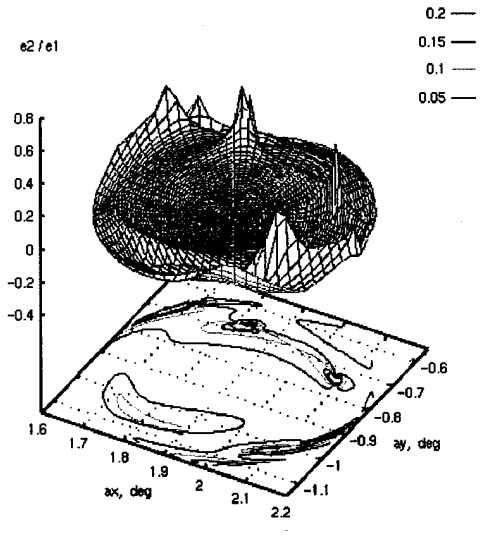

Fig. 6: Ratio of the minor-to-major axes of the polarization ellipse

An important technical question to be answered about the polarization properties of the telescope is how the polarization of the beam changes in response to a rotation of the field polarization vector $\vec{e}_0$ on the horn aperture (i.e., in response to twisting the polarizer about the horn axis).

The answer is that the beam polarization rotates basically in the same way, i.e., the major axes of the polarization ellipses at the central part of the beam rotate by the same angle about the observation directions as the vector $\vec{e}_0$ on the horn aperture about the horn axis. In the meantime, the spatial structure of the patterns shown above remains approximately the same.

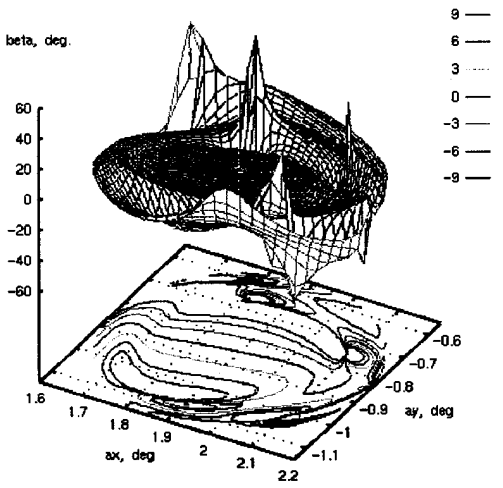

Fig. 7: Phase delay of the minor-axis component with respect to the major-axis one

Concluding the analysis of the properties of the H-143-4 beam, Fig. 8 shows the defocusing effect of the horn on the gain function G defined as

$$G = 10\log_{10}(4\pi P(0)/P) \tag{4}$$

where $P(0)$ is the power flux on the beam axis and $P = 1$ is the total power of the beam. The position of the horn is specified by the refocus parameter R_A, which is similar to R_F but measured to the centre of the horn aperture.

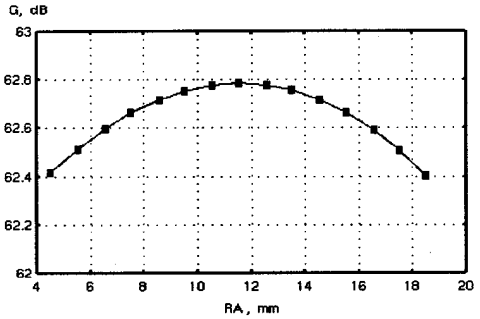

Fig. 8: Defocusing effect of the horn H-143-4

For the Gaussian horn with a plane phase front at the aperture, the optimum value of R_A is expected to be about R_F. Indeed, Fig. 8 shows that the optimum position is only 1 mm = 0.5λ ahead of the geometrical focus R_F, and the variation of G is sufficiently small, being only 0.4 dB within the range of ± 7 mm that is $\pm 3.5\lambda$ around the optimum point.

4. Beam from the Multi-Moded Horn H-545-1

Multi-moded horns are designed for receiving maximum microwave power within the required angular resolution consistent with the requirements on the beam taper at the secondary mirror of a level of –30 dB, with an aspect angle of 25 degrees. These are rather restrictive and contradictory requirements resulting in the big aperture area of the corrugated conical horns specially optimized for the given application [2].

Since the phase front of the aperture field is convex, the effective focal centre is located inside the horn at a distance R_C from the aperture. Parameter R_C can be estimated by considering the basic mode of the horn field as a Gaussian beam propagating through the horn aperture.

For the horn H-545-1, the estimate is $R_C = 18.7$ mm, with the Gaussian half-width $w = 2.639$ mm at the horn aperture and the half-waist $w_0 = 1.519$ mm at the effective focal centre.

The horn is supposed to be properly focused if the aperture refocus parameter is $R_A = R_F + R_C = 24.2$ mm. In this case one should expect the far field of the telescope to be just a map of the aperture field.

Since the total aperture field is a non-coherent superposition of all the modes propagating through the horn, no phase is associated with the beam, even though the total power pattern is approximately Gaussian.

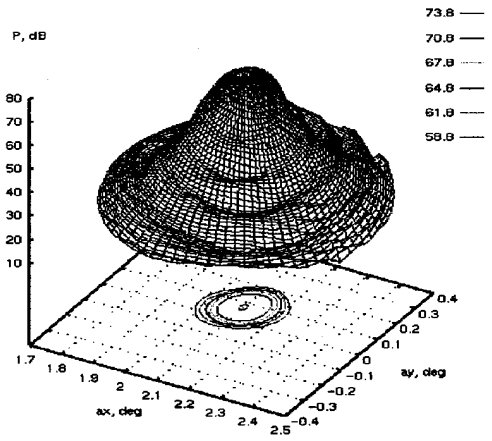

Fig. 9: Power pattern of the telescope beam from the multi-moded horn H-545-1 placed at the estimated refocus $R_A = 24$ mm

The full width of the telescope beam at –4.3 dB can be estimated roughly as $W = 2Mw = 9.08$ arcmin where $M = 1.72$ arcmin/mm is the geometrical magnification of the telescope. The estimate assumes, as a kind of natural approximation, a uniform phase assigned to the incoherent field at the horn aperture. The full width of the basic mode projected on the sky is estimated more rigorously as $W_0 = 2Mw_0 = 5.22$ arcmin.

The power pattern of the telescope beam computed for the multi-moded horn H-545-1 is shown in Fig. 9. One can see that the beam on the sky is well shaped and has a flat top but it is much too wide. The edge of the flat top is just about –3 dB below the maximum. The full beam width at the edge is found to be $W_{min} = 8.0$ arcmin and $W_{max} = 9.8$ arcmin which is quite close to the estimate above but almost twice greater than the required resolution of 5 arcmin.

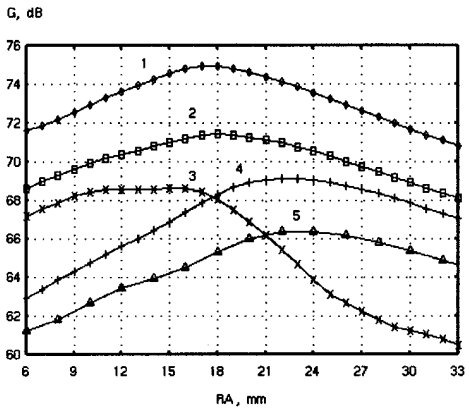

Fig. 10: Defocusing effect of the horn H-545-1:
1- 6 modes (m = 1 – 6, all polarizations),
2- 2 modes (m = 1, 6), 3- m = 6,
4- basic mode (m = 1), 5- Gaussian beam

In order to find the optimum position of the horn, we studied the defocusing effect over a wide range of the refocus parameter R_A, Fig. 10.

In Fig. 10, the gain G is defined in a similar way to (4) but assuming that $P(0)$ is the on-axis flux of the total power of all the modes in both polarizations and $P = 1$ is the power of a single mode.

Fig. 10 clearly shows that, for the Gaussian beam approximating the basic mode, the optimum refocus parameter is, indeed, $R_A = 24.2$ mm as estimated above. However, the optimum refocus of the multi-moded horn is $R_A = 17.5$ mm, i.e., by 12λ less than the estimate above which results in an increase of gain by 1.5 dB providing $G_{\max} = 75$ dB.

The effect arises due to the aberrations of the telescope which cause, on defocusing the horn, such a distortion of different modes that they compensate each other at the edge of the beam and better collect the power of all the modes right at the beam axis.

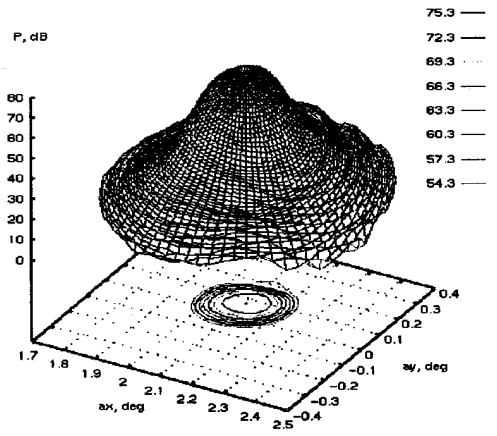

Fig. 11: Power pattern of the horn H-545-1 placed at $R_A = 17.5$ mm providing $G_{\max} = 75$ dB

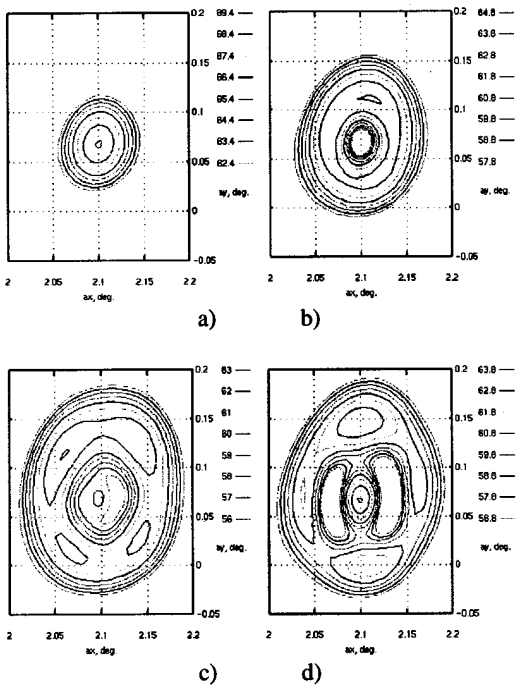

Fig. 12: Power patterns of different modes: (a) m=1; (b) m=2,3; (c) m=4,5; (d) m=6 ($R_A = 24$ mm)

The beam pattern computed at the optimum refocus of the multi-moded horn ($R_A = 17.5$ mm) is shown in Fig. 11. In this case, the total power of the beam is concentrated in a smaller area resulting in the increase of gain observed in Fig. 10.

Figures 12 and 13 show the patterns of separate modes at different values of the refocus parameter R_A. They illustrate the mechanism of increasing the gain by playing with aberrations as discussed above.

The beam obtained at the optimum refocus is still slightly flat topped, although the top is not so perfectly shaped. The effective width of the beam at the edge of the flat top (at –3 dB) varies from $W_{\min} = 6.8$ arcmin to $W_{\max} = 7.8$ arcmin. It is less than in the previous case but still about 1.5 times greater than the desired angular resolution of the telescope at the given frequency. Further optimization of the multi-moded horns is expected to improve the resolution by means of filling the margins of the beam taper at the secondary mirror that still exists in the model considered.

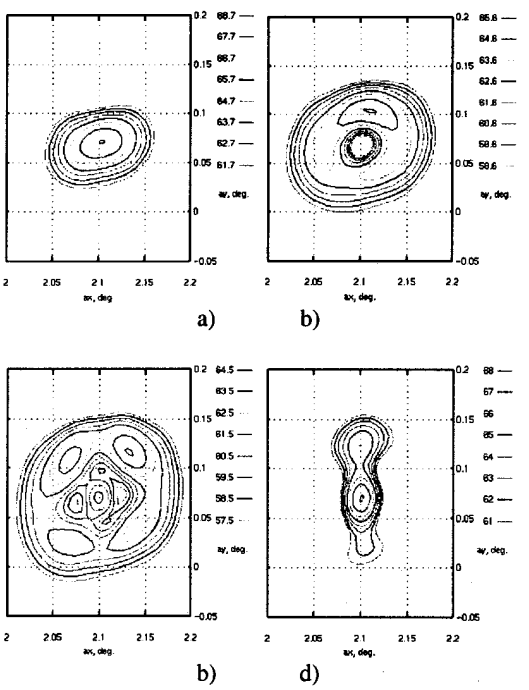

Fig. 13: Power patterns of different modes: (a) m=1; (b) m=2,3; (c) m=4,5; (d) m=6 ($R_A = 17.5$ mm)

5. Conclusion

A fast physical optics simulator has been developed for the analysis of the dual-reflector submillimeter-wave telescope on the ESA Planck Surveyor. The code overcomes the limitations of a generic approach for large multi-reflector quasi-optical systems and can perform typical simulations of the telescope in the order of minutes.

A study of the power patterns, polarization characteristics, defocusing effects and modal structure of the telescope beams from both the Gaussian and multi-moded horns operating at 143 and 545 GHz, respectively, has been performed.

Analysis of the beams from the linearly polarized Gaussian horns have shown that the far-field of the telescope is, generally, elliptically polarized except precisely at the beam axis where linear polarization is preserved.

When rotating the polarization vector of the horn field about the horn axis, the major axes of the polarization ellipses at the central part of the telescope beam rotate by the same angle about the direction of observation. At the same time, the power patterns of both the co- and cross-polarized components of the far field remain basically unchanged.

Even for the most tilted Gaussian horns operating at the frequency of 143 GHz, the power associated with the minor axes of the polarization ellipses in the telescope beam remains at the level of about 40 dB below the maximum power of the beam.

In order to achieve maximum angular resolution with multi-moded horns, the latter should be located slightly further from the secondary mirror compared to the estimates based on the Gaussian approximation applied to the optimal focal positions as found by the ray tracing techniques.

Acknowledgement

The authors are grateful to Yuying Longval for providing updated positions and aiming angles of the high-frequency horns. V.Y. and J.A.M. would like to acknowledge the support of Enterprise Ireland.

References

1. http: // astro.estec.esa.nl / Planck
2. R. Colgan, J. A. Murphy, B. Maffei, C. O'Sullivan, R. Wylde, P. Ade, "Modelling Few-Moded Horns for Far-IR Space Applications", to appear in the 11th Int. Symp. on Space Terahertz Technology, 2000
3. L. Diaz, T. Milligan, Antenna Engineering Using Physical Optics: Practical CAD Techniques and Software, Artech House, London, 1996
4. C. Scott, Modern Methods of Reflector Antenna Analysis and Design, Artech House, London, 1990
5. http: // astro.estec.esa.nl / Planck / pictures / pictures_top.html